IJE TRANSACTIONS B: Applications Vol. 28, No. 11, (November 2015) 1589-1596

International Journal of Engineering

Journal Homepage: www.ije.ir

A Robust Image Denoising Technique in the Contourlet Transform Domain

E. Ehsaeyan

Faculty of Sirjan University of Technology, electrical engineering Department, Sirjan, Iran

PAPER INFO

Paper history:
Received 17 August 2015
Received in revised form 15 October 2015
Accepted 19 November 2015

Keywords:
Denoising, Contourlet Transform
Bilateral Filter
SURE Shrink
Multiresolution Analysis
Universal Index
Image Fidelity
Mean Square Error

ABSTRACT

The contourlet transform can very well capture the directional geometrical structures of natural images. In this paper, by incorporating the ideas of Stein's unbiased risk estimator (SURE) approach in nonsubsampled contourlet transform (NSCT) domain, a new image denoising technique is devised. We utilize the properties of NSCT coefficients in high and low subbands and apply SURE shrinkage and bilateral filter respectively. Moreover, SURE-LET strategy is modified to minimize the estimation of the mean square error (MSE) between the clean image and the denoised one in the NSCT domain. The simulation testing has been carried on under the different noise level, and the denoising effect has been evaluated by using the peak signal to noise ratio (PSNR). Results for different kinds of sample image show that the introduced algorithm in this paper can maintain most important details of images, remove Gaussian white noise more effectively, and get a higher PSNR value, which also has a better visual effect.

doi: *10.5829/idosi.ije.2015.28.11b.06*

1. INTRODUCTION

Nowadays, the image enhancement and image restoration are essential processes in practical applications [1-5]. For example, corrupted by additive white Gaussian noise (AWGN) is a common problem in the image processing and video coding, which are created by noisy environment and reduces the performance of systems.

A study of denoising optical coherence tomography (OCT) heart tube image based on the contourlet transform and the exploration of the coefficient inter-direction dependency has been presented and the variance of the noise in log-domain has been derived [6]. A novel denoising framework with the direction statistic based on Improved Rotating Kernel Transformation has been reported [7]. The method had a good performance in denoising medical images by introducing a new thresholding framework. A suppressing speckle noise scheme has been carried out for SAR images [8]. This method worked within the outline of the multiscale nonsubsampled contourlet transform (NSCT) and memetic algorithm (MA) with the ability of preserving salient features and adjusting the detail contrast.

Yan et al. have adopted an optimized directional filter bank in contourlet transform to overcome the redundancy of this transform and introduced a fast nonsubsampled contourlet algorithm for image denoising, image fusion and similar applications [9]. A despeckling method for ultrasound medical images based on non-subsampled contourlet transform has been presented [10]. This algorithm utilized binary morphological operations and the advantages of shift invariant and directionality of NSCT to preserve details. Min et al. have developed contourlet transform and introduced a novel structure named dual contourlet transform (DCT) [11]. They combined dual tree complex wavelet transform (DTCWT) and contourlet transform to achieve a new transform with shift invariant and higher directional selectivity characteristics. A new algorithm in denoising synthetic aperture radar (SAR) images with combining nonsubsampled contourlet transform (NSCT) and affinity, which could preserve details in smoothing homogeneous regions, has been proposed [12].

*Corresponding Author's Email: ehsaeyan@sirjantech.ac.ir (E. Ehsaeyan)

Please cite this article as: E. Ehsaeyan, A Robust Image Denoising Technique in the Contourlet Transform Domain, International Journal of Engineering (IJE), TRANSACTIONS B: Applications Vol. 28, No. 11, (November 2015) 1589-1596

In this paper, a new contourlet domain image denoising framework based on SURE shrink and bilateral filter has been presented. The new algorithm combined the good properties of the non-subsampled Contourlet transform, SURE shrink and bilateral filter in the image denoising issue. Bilateral filter is used to refine low frequency band and SURE-LET approach is used to shrink noisy data in highpass subbands. We apply a modified model of SURE shrink with optimal threshold and window size to achieve better results.

The rest of the paper is organized as follows. In Section 2, the basic concepts of contourlet transform, SURE shrinkage and bilateral filter are introduced. In Section 3, the proposed denoising scheme is presented and details of implementation are provided. Section 4 describes experimental results about the standard images of our algorithm. In this section, a performance comparison of the introduced method over other up-to-date denoising techniques, is presented. At the end, Section 5 concludes the paper.

2. BASIS THEORY

2. 1. Contourlet By combining the Laplacian Pyramid (LP) and the directional filter bank (DFB), Do and Vetterli proposed the contourlet transform (CT) [13], which decomposes the spectrum into trapezoid-shaped subbands, as shown in Figure 1.

The generation of the contourlet transform is illustrated in Figure 2, where a one-level LP decomposes an input image into a downsampled low-pass subband and a highpass subband. Then, the highpass subband are decomposed into various directional subbands by the DFB.

To avoid the division of low frequency regions, at each stage, the contourlet transform removes the low frequency component from the highpass subband before implementing the DFB decomposition. If this procedure is iterated on the lowpass subband, then a multiscale and multidirection decomposition of images is achieved. By taking the advantages of both the LP and the DFB, the contourlet transform can efficiently capture high frequency directional information in images, such as oriented edges. A possible frequency partition by the contourlet transform is illustrated in Figure 1, by which the spectrum of an original image could be decomposed into four scales. Based on the frequency partition shown in Figure 1, the coefficient image resulting from the contourlet transform applied to a test image is shown in Figure 3, in which the coefficients with small absolute value are black. Due to the abundant number of small-absolute-value coefficients, the contourlet transform is a sparse expression of images. Each subband of the contourlet transform which consists of a pairwise trapezoid-shaped regions symmetric to the origin in Figure 1, corresponds to an oriented basis function.

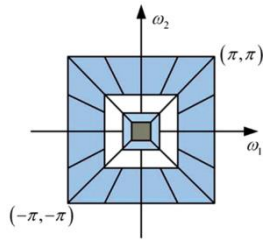

Figure 1. Frequency partition, in which the spectrum of an image is decomposed into four pyramid levels (indicated by the shades of gray, blue and white)

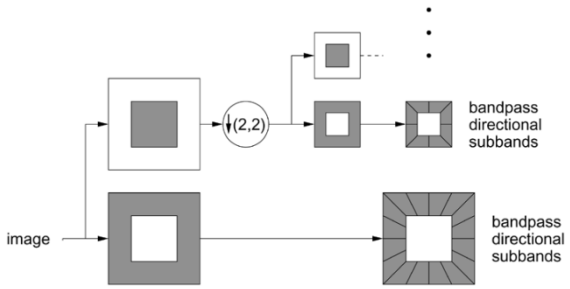

Figure 2. Illustration of the contourlet transform in the 2-D frequency domain, where the LP decomposes the frequency spectrum of an original image into multi-scales. Then each bandpass scale is decomposed into directional subbands by the DFB. (Based on a figure from [13])

Therefore, the contourlet transform can offer basis functions oriented at $2k$ different directions at each scale, where k is an arbitrary positive integer. Rich and flexible multiscale and oriented basis functions allow the contourlet transform to effectively represent smooth contours.

2. 2. Sure Shrinkage Suppose there is an (noisy) observed 2D gray image signal as:

$$I_{in}(s) = I_{real}(s) + n(s) \quad , s \in T \tag{1}$$

where $I_{real}(s)$ is the deterministic 2D gray image signal and $n(\mathbf{s})$ is an independent and identical distributed (i.i.d.) Gaussian noise with mean zero and covariance σ^2 , and T is the set of spatial indices of the whole image ($T \triangleq [T_1, T_2, \dots, T_{HL}]$) .The total number of pixels in the image is HL. Suppose $I_{out,\theta}(s)$ is an estimate of $I_{real}(s)$ obtained from $I_{in}(s)$ as:

$$I_{out,\theta}(s) = f(I_{in}(s), \theta) = f(I_{real}(s) + n(s), \theta), \ s \in T \tag{2}$$

where f is an estimator (possibly nonlinear) of $I_{real}(s)$ and θ is a parameter vector associated with this estimator. The goodness of the estimator f can be measured using sample mean square error (MSE) measure expressed as

$$MSE = \frac{1}{HL}\sum_{s\in T}\left[\left\|I_{out,\theta}(s) - I_{real}(s)\right\|^2\right] \tag{3}$$

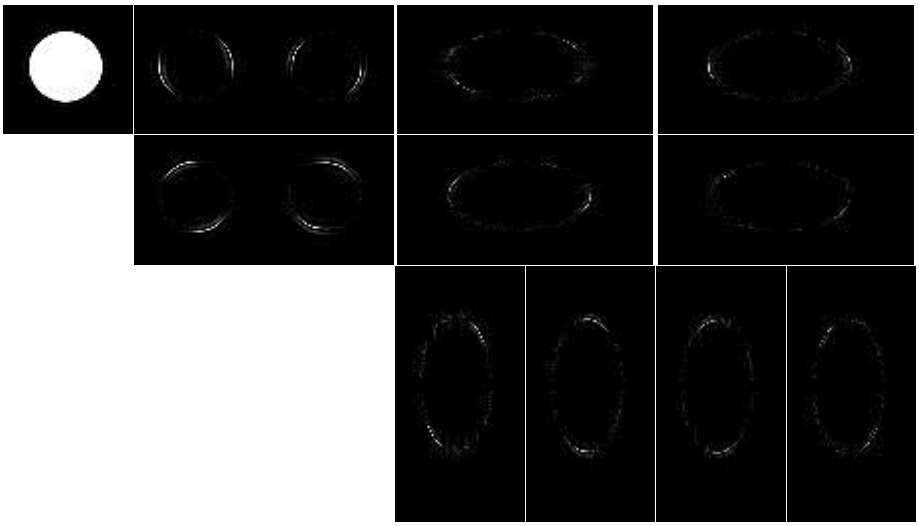

Figure 3. Contourlet transform of the Test image. The image is decomposed into two pyramidal levels, which are then decomposed into four and eight directional subbands. Small coefficients are showed by black while large coefficients are showed by white

One of the problems in using this criterion to the corrupted image is that the noise-free image, $I_{real}(s)$, is not available. This measuring parameter depends on the amount of the noise of the observed image. Risk R_θ is defined the expected value of Mean Square Error as:

$$R_\theta = \mathbf{E}[MSE] \tag{4}$$

Although, it is not possible to access the Risk parameter without the unknown original image, however, this drawback has been solved by Stein's Unbiased Risk Estimator (SURE) technique [14, 15]. With the assumption of AWGN noise distribution, SURE provides an analytical means for unbiased estimation of Mean Square Error. It is given by:

$$\hat{R}_\theta = \frac{1}{HL}\sum_{s\in T}\left[\left\|I_{in}(s) - I_{out,\theta}(s)\right\|^2\right] - \sigma^2 + 2\sigma^2\frac{1}{HL}\sum_{s\in T}\left[\frac{\partial f(I_{in}(s),\theta)}{\partial I_{in}(s)}\right] \tag{5}$$

To obtain the best answer, we regard $\hat{R}_\theta$ as a reliable estimate of the Mean Square Error, which is mentioned in Equation (5). HL denotes the size of the observed image. If we know σ^2 (or estimate it separately), then we can calculate $\hat{R}_\theta$ and minimize it with respect to θ to find the optimum parameters of the signal estimator in Equation (2).

2. 3. Bilateral Filter Bilateral filter is a useful non-linear noise reduction filter which can preserve details without smoothing the images. This filter acts like median filter. In this different that the intensity of centric pixel in an image is substituted by a weighted average of neighbor pixels with specified window size. One of the solutions to calculated weights is Gaussian distribution. Specially, these values depend on distance and intensity of pixels. The process of edge preserving is done with adjusting the weights in a loop manner automatically. According to definition, the bilateral filter is mentioned as [16]:

$$I_{filtered}(x) = \frac{1}{W_p}\sum_{x_i\in\Omega} I(x_i) f_r(||I(x_i) - I(x)||) g_s(||x_i - x||) \tag{6}$$

where:

$$W_p = \sum_{x_i\in\Omega} f_r(||I(x_i) - I(x)||) g_s(||x_i - x||) \tag{7}$$

In this equation, $I_{filtered}$ is the output image, I the main image which must be filtered, x the location of the centric pixel, Ω the window which centered in a pixel with coordination of x and f_r such as Gaussian function that is the range kernel for smoothing of the intensity. g_s such as Gaussian function, is the spatial kernel for smoothing.

3. PROPOSED METHOD

In this section, we discuss implementation details of the proposed method. Figure 4 illustrates the block diagram of the proposed scheme. The specific procedure of proposed denoising method based on SURE shrink and bilateral filter in NSCT domain, is as follows: First, the nonsubsampled contourlet transform (NSCT) is used to obtain a multiscale and multidirectional decomposition of the noisy image. NSCT is selected due to the property of high directionality, anisotropy and

translation invariance. Second, the lowpass subband and other band directional subband are separated. For the highpass subbands and low frequency subband, SURE shrinkage and bilateral filter are used to denoising coefficients respectively. There is a little noise in the low-frequency band, and after the bilateral filter processing, the noise is reduced. Hence, the low-frequency band need not be refined with SURE shrink processing.

We modify SURE-LET approach to minimize the estimation of the Mean Square Error (MSE) between the clean image and the denoised one in the NSCT domain. As suggested in [17], we apply optimal threshold and window size to highpass bands. In our procedure, window sizes of 3×3 and 5×5 and 15 threshold points considered near Universal threshold [18] are examined to yield best minimum MSE parameter for each subband. In other words, every subband is denoised independently. In the each level, the window size is checked to reach the maximum L_{max}. This parameter is set to five in our algorithm. We noticed that the window size 3×3 and 5×5 approximately satisfy the RISK condition. So, we do not spend time to check the higher order of the window size. After these processes, the nonsubsampled contourlet inverse transform is done and the reconstructed image after the procedure of sub-band coefficients is rebuilt and the restore image is gotten.

4. RESULTS AND DISCUSSION

In this section, we compare the proposed method with other denoising methods. We have performed several experiments to test the proposed algorithms and evaluate its performance with standard images. The performance of the method was evaluated by measuring the peak signal-to-noise ratio (PSNR). For the contourlet transform as suggested in [19], we use the '*maxflat*' filters with two levels of pyramidal decomposition for the multiscale decomposition stage and partition the finest scale to eight directional subbands. The denoising results of the House image are depicted in Figure 5.

The visual results show that the introduced algorithm preserves the integrity of edge and detail information and produces the good quality in the standpoint of perceptual view.

The performance of the proposed scheme is compared to five well-known denoising methods: ProbShrink, BLS-GSM, SUREbivariate, NL-means and Total Variation (TV) model. For this study, we use three benchmark images named House, Barbara and Cameraman (8-bit grayscale, size 512×512 and 256×256) taken from database [1]. The noisy images are obtained by adding Gaussian white noise (noise standard deviations ranging from 20 to 70) to the noise-free image. The results are shown in Table 1 and Figure 6. The results confirm that the proposed method gives highest PSNR for all the experimented images and has a better noise suppression in the visual comparison. Comparative PSNR results are presented in Table 2, where the proposed framework is compared with wavelet-domain spatially adaptive BayesShrink thresholding with square window (wavelet SABS-SW) [20], the contourlet-domain spatially adaptive BayesShrink thresholding with the square window (contourlet SABS-SW), the denoising method based on the contourlet-domain contextual hidden Markov model (contourlet CHMM) [21] and Local thresholding with adaptive window shrinkage in the contourlet domain (contourlet Local-Th) [22].

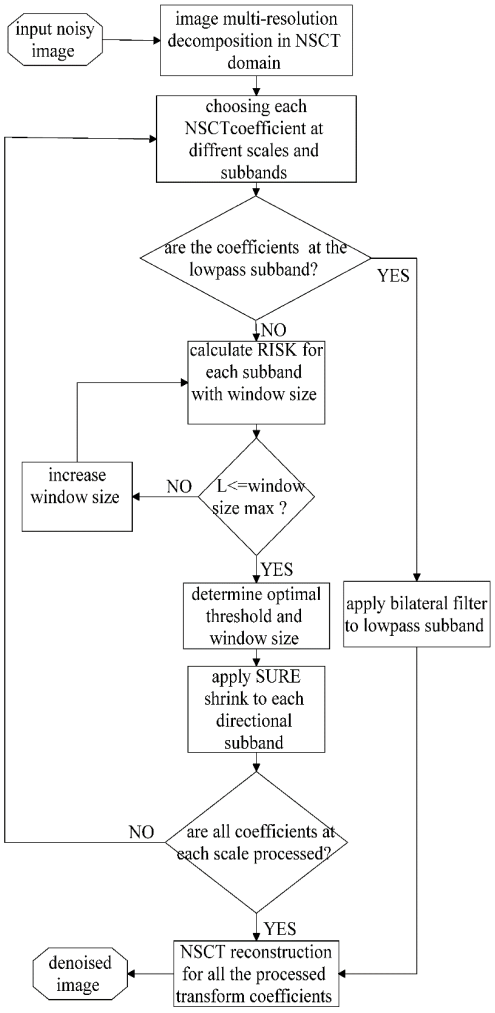

Figure 4. Proposed denoising framework

1. http://www.imageprocessingplace.com/root_files_V3/image_databases.htm

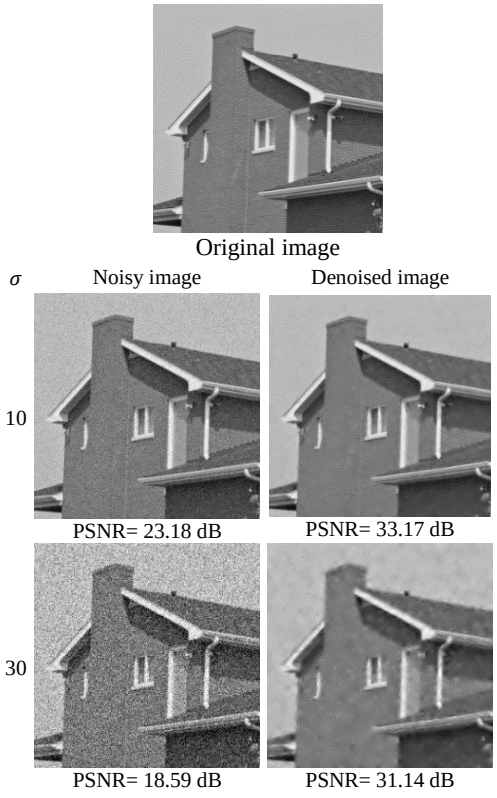

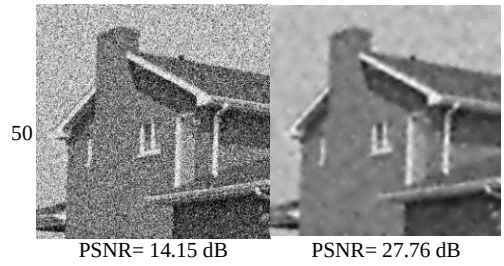

Figure 5. The visual denoising results of proposed method. First column indicates noisy images. Second column is denoised images by applying proposed algorithm

From data in Table 2, it is clear that the introduced denoising scheme is better than the other denoising methods in most cases.

At the same time, to interpret the advantage of introduced algorithm, the denoised results of the images Lena, Barbara and Peppers obtained by recent state-of-art methods are also shown in Table 3. The highest PSNR in every column is bolded. Again, we can see that the noisy images are better recovered using the proposed approach compared to other methods.

Figure 6. visual results of different denoising methods and proposed algorithm for image Barbara: a) original image, b) the noisy image with $\sigma = 30$, c) denoised by ProbShrink, d) denoised by BLS-GSM, e) denoised by SUREbivariate f) denoised by NL-means, g) denoised by TV model, h) denoised by proposed method

TABLE 1. PSNR performance comparison of different well-known denoising methods

σ	**20**	**30**	**40**	**50**	**60**	**70**
Input PSNR	22.11	18.59	16.09	14.15	12.57	11.23
Method			House (256 × 256)			
ProbShrink [23]	30.29	28.35	27.14	25.99	25.50	24.28
BLS-GSM [24]	30.79	28.72	27.44	26.15	25.62	25.02
SUREbivariate [25]	30.93	28.96	27.61	26.58	25.78	25.10
NL-means	30.56	27.79	26.09	24.99	24.23	23.68
TV model	30.74	28.96	27.65	26.42	25.46	24.57
Our method	31.14	29.17	27.76	26.61	25.8	25.14
Method			Barbara (512 × 512)			
ProbShrink [23]	28.40	26.27	24.89	23.86	23.32	21.99
BLS-GSM [24]	28.28	25.92	24.44	23.50	22.87	22.39
SUREbivariate [25]	27.98	25.83	24.54	23.70	23.15	22.72
NL-means	27.42	24.16	23.69	22.57	21.89	21.64
TV model	26.32	24.73	23.85	23.17	22.79	22.31
Our method	29.60	27.33	25.73	24.39	23.41	22.97
Method			Cameraman (256 × 256)			
ProbShrink [23]	28.25	26.13	24.78	23.80	22.83	22.13
BLS-GSM [24]	28.29	26.24	24.94	24.03	23.00	22.30
SUREbivariate [25]	28.51	26.48	25.11	24.10	23.29	22.63
NL-means	27.59	25.23	23.44	22.28	21.51	20.98
TV model	27.91	26.12	24.98	24.02	23.10	22.48
Our method	29.04	26.97	25.38	24.27	23.3	22.39

TABLE 2. Comparison of the denoised images obtained from the different methods. These results were published in [22] and were directly imported from it.

Image 512×512	**Noise level**	**PSNR**				
		Wavelet SABS-SW	Contourlet SABS-SW	Contourlet CHMM	Contourlet Local-Th	Proposed method
Lena	15	31.01	31.12	31.75	32.59	**33.2**
	20	29.59	29.37	30.62	31.25	**31.6**
	25	28.51	27.95	29.59	30.20	**30.6**
	30	27.54	26.76	28.76	29.35	**29.56**
Barbara	15	28.48	29.77	29.68	30.55	**31.45**
	20	27.02	27.97	28.52	29.03	**29.60**
	25	25.90	26.57	27.33	27.88	**28.02**
	30	25.01	25.40	26.47	26.98	**27.33**
Peppers	15	30.62	30.86	31.23	32.05	**32.53**
	20	29.29	29.17	30.19	30.84	**31.18**
	25	28.30	27.81	29.21	29.87	**30.24**
	30	27.53	26.64	28.44	**29.7**	29.34

TABLE 3. Performance comparisons of different denoising methods in term of PSNR

	Lena		**Barbara**		**Peppers**	
σ	20	30	20	30	20	30
[26]	30.77	29.04	28.55	**27.38**	30.57	28.83
[27]	30.92	29.13	28.48	26.27	30.57	28.83
[28]	28.25	25.7	26.81	24.49	26.96	25.03
[29]	31.16	29.25	28.71	26.59	30.81	28.92
[30]	30.61	28.73	26.57	26.36	29.31	27.85
[31]	30.42	28.54	26.28	24.73	30.17	28.28
Our work	**31.6**	**29.56**	**29.60**	27.33	**31.18**	**29.34**

5. CONCLUSION

In this paper, we have introduced a robust image denoising technique in the contourlet transform domain. In various multi-scale geometric analysis methods, we chose the NSCT because of its properties of fully shift-invariant, multi-scale, multidirection and can be easily implemented. With this method, the resulted image upon denoising is obtained within the framework of Unbiased Risk Estimator (SURE) estimation in high frequency area and bilateral filter in the low frequency band. We present some numerical results to show the reliability of our method. Experiments in different kinds of sample images demonstrate the effectiveness of the proposed method and show the superiority to previous image denoising methods such as Wavelet SABS-SW, Contourlet SABS-SW, Contourlet CHMM and contourlet Local-Th in objective and subjective qualities. Further, improvements in this algorithm will be suggested in the near future to deal with other kinds of noises in image processing.

6. REFERENCES

1. Khosravi, M. and Hassanpour, H., "Image denoising using anisotropic diffusion equations on reflection and illumination components of image", ***International Journal of Engineering-Transactions C: Aspects***, Vol. 27, No. 9, (2014), 1339-1348.
2. Nadernejad, E., Hassanpour, H. and Miar, H., "Image restoration using a pde-based approach", ***International Journal of Engineering Transactions B: Applications***, Vol. 20, No. 3, (2007).
3. Keyvanpour, M., Tavoli, R. and Mozafari, S., "Document image retrieval based on keyword spotting using relevance feedback", ***International Journal of Engineering-Transactions A: Basics***, Vol. 27, No. 1, (2013), 7-14.
4. Farbiz, F., Menhaj, M. and Motamedi, S., "A new iterative fuzzy-based method for image enhancement", ***International Journal of Engineering***, Vol. 13, No. 3, (2000), 69-74.
5. Hassanpour, H. and Ghadi, A.R., "Image enhancement via reducing impairment effects on image components", ***International Journal of Engineering-Transactions B: Applications***, Vol. 26, No. 11, (2013), 1267-1274.
6. Guo, Q., Dong, F., Sun, S., Lei, B. and Gao, B.Z., "Image denoising algorithm based on contourlet transform for optical coherence tomography heart tube image", ***Image Processing, IET***, Vol. 7, No. 5, (2013), 442-450.
7. Guo, Q., Dong, F., Sun, S., Ren, X., Feng, S. and Gao, B.Z., Improved rotating kernel transformation based contourlet domain image denoising framework, in Advances in multimedia information processing–PCM 2013, (2013), Springer ,146-157.
8. Li, Y., Hu, J. and Jia, Y., "Automatic sar image enhancement based on nonsubsampled contourlet transform and memetic algorithm", ***Neurocomputing***, Vol. 134, (2014), 70-78.
9. Chun-Man, Y., Bao-Long, G. and Meng, Y., "Fast algorithm for nonsubsampled contourlet transform", ***Acta Automatica Sinica***, Vol. 40, No. 4, (2014), 757-762.
10. Babu, J.J.J. and Sudha, G.F., "Non-subsampled contourlet transform based image denoising in ultrasound thyroid images using adaptive binary morphological operations", ***IET Computer Vision***, Vol. 8, No. 6, (2014), 718-728.
11. Min, D., Jiuwen, Z. and Yide, M., "Image denoising via bivariate shrinkage function based on a new structure of dual contourlet transform", ***Signal Processing***, Vol. 109, (2015), 25-37.
12. Tian, X., Jiao, L. and Guo, K., "An affinity-based algorithm in nonsubsampled contourlet transform domain: Application to synthetic aperture radar image denoising", ***Journal of Signal Processing Systems***, (2015), 1-16.
13. Do, M.N. and Vetterli, M., "The contourlet transform: An efficient directional multiresolution image representation", ***Image Processing, IEEE Transactions on***, Vol. 14, No. 12, (2005), 2091-2106.
14. Stein, C.M., "Estimation of the mean of a multivariate normal distribution", ***The Annals of Statistics***, (1981), 1135-1151.
15. Solo, V., "A sure-fired way to choose smoothing parameters in ill-conditioned inverse problems", in Image Processing, Proceedings., International Conference on, IEEE. Vol. 3, (1996), 89-92.
16. Tomasi, C. and Manduchi, R., "Bilateral filtering for gray and color images", in Computer Vision. Sixth International Conference on, IEEE, (1998), 839-846.
17. Dengwen, Z. and Wengang, C., "Image denoising with an optimal threshold and neighbouring window", ***Pattern Recognition Letters***, Vol. 29, No. 11, (2008), 1694-1697.
18. Donoho, D.L. and Johnstone, J.M., "Ideal spatial adaptation by wavelet shrinkage", ***Biometrika***, Vol. 81, No. 3, (1994), 425-455.
19. Da Cunha, A.L., Zhou, J. and Do, M.N., "The nonsubsampled contourlet transform: Theory, design, and applications", ***Image Processing, IEEE Transactions on***, Vol. 15, No. 10, (2006), 3089-3101.
20. Chang, S.G., Yu, B. and Vetterli, M., "Adaptive wavelet thresholding for image denoising and compression", ***Image Processing, IEEE Transactions on***, Vol. 9, No. 9, (2000), 1532-1546.
21. Long, Z. and Younan, N.H., "Statistical image modeling in the contourlet domain using contextual hidden markov models", ***Signal Processing***, Vol. 89, No. 5, (2009), 946-951.
22. Shen, X., Wang, K. and Guo, Q., "Local thresholding with adaptive window shrinkage in the contourlet domain for image denoising", ***Science China Information Sciences***, Vol. 56, No. 9, (2013), 1-9.
23. Pizurica, A. and Philips, W., "Estimating the probability of the presence of a signal of interest in multiresolution single-and multiband image denoising", ***Image Processing, IEEE Transactions on***, Vol. 15, No. 3, (2006), 654-665.
24. Portilla, J., Strela, V., Wainwright, M.J. and Simoncelli, E.P., "Image denoising using scale mixtures of gaussians in the wavelet domain", ***Image Processing, IEEE Transactions on***, Vol. 12, No. 11, (2003), 1338-1351.
25. Luisier, F., Blu, T. and Unser, M., "A new sure approach to image denoising: Interscale orthonormal wavelet thresholding", ***Image Processing, IEEE Transactions on***, Vol. 16, No. 3, (2007), 593-606.
26. Om, H. and Biswas, M., "A generalized image denoising method using neighbouring wavelet coefficients", ***Signal, Image and Video Processing***, Vol. 9, No. 1, (2015), 191-200.
27. Om, H. and Biswas, M., "Mmse based map estimation for image denoising", ***Optics & Laser Technology***, Vol. 57, (2014), 252-264.
28. Jain, P. and Tyagi, V., "An adaptive edge-preserving image denoising technique using tetrolet transforms", ***The Visual Computer***, Vol. 31, No. 5, (2014), 657-674.

29. Biswas M. and Om H., "A new adaptive image denoising method based on neighboring coefficients", ***Journal of The Institution of Engineers (India): Series B***, (2014), 1-9.

30. Tian, D., Xue, D. and Wang, D., "A fractional-order adaptive regularization primal–dual algorithm for image denoising", ***Information Sciences***, Vol. 296, (2015), 147-159.

31. He, N., Wang, J.-B., Zhang, L.-L. and Lu, K., "An improved fractional-order differentiation model for image denoising", ***Signal Processing***, Vol. 112, (2015), 180-188.

A Robust Image Denoising Technique in the Contourlet Transform Domain

E. Ehsaeyan

Faculty of Sirjan University of Technology, electrical engineering Department, Sirjan, Iran

P A P E R I N F O

Paper history:
Received 17 August 2015
Received in revised form 15 October 2015
Accepted 19 November 2015

Keywords:
Denoising, Contourlet Transform
Bilateral Filter
SURE Shrink
Multiresolution Analysis
Universal Index
Image Fidelity
Mean Square Error

چکیده

تبدیل کنتورلت قابلیت توصیف ساختارهای هندسی جهت‌دار را در تصاویر به‌طور ویژه دارا می باشد. در این مقاله با به کارگیری ایده تخمین ریسک Stein (SURE) در یک حوزه تبدیل کنتورلت به نام تبدیل کنتورلت تغییرناپذیر با مکان NSCT، یک روش برای حذف نویز از تصاویر خاکستری ارائه شده است. در این مقاله ما از خصوصیات ضرایب تبدیل کنتورلت NSCT در باندهای بسامدی بالا و پایین استفاده و روش حذف نویز SURE و فیلتر دوسویه را به ترتیب بر این ضرایب اعمال می‌کنیم. علاوه بر این، به منظور بهبود کاهش پارامتر حداقل مربعات خطا (MSE) در محاسبات ریسک، تکنیک SURE-LET را بین تصویر اصلی و تصویر بازیابی شده در حوزه تبدیل کنتورلت NSCT تغییر می دهیم. نتایج شبیه‌سازی در حالات مختلف نویز ارائه و کارایی الگوریتم پیشنهادی توسط پارامتر نسبت حداکثر سیگنال به نویز PSNR ارزیابی می‌شود. نتایج حاصل از تصاویر مختلف استاندارد حاکی از آن است که طرح‌واره پیشنهادی در این مقاله توانایی حفظ اطلاعات تصویر و حذف نویز گوسی سفید را به طور موثری داراست. درحالی که تصاویر رفع نویز شده، شاخص PSNR بالاتر و وضوح ظاهری بهتری بعد از فرایند رفع نویز توسط الگوریتم پیشنهادی دارند.

***doi**: 10.5829/idosi.ije.2015.28.11b.06*